Cryoenzymology of *Bacillus cereus* β-Lactamase II†

Roy Bicknell‡ and Stephen G. Waley*
Sir William Dunn School of Pathology, University of Oxford, Oxford OX1 3RE, U.K.
Received February 1, 1985

ABSTRACT: The effects of cryosolvents and subzero temperatures on the metalloenzyme β-lactamase II from *Bacillus cereus* have been investigated. Preliminary experiments led to the selection of suitable systems for the study of β-lactamase II catalysis at low temperatures, namely, cobalt(II) β-lactamase II hydrolysis of benzylpenicillin in 60% (v/v) ethylene glycol and zinc β-lactamase II hydrolysis of the chromophoric cephalosporin nitrocefin in 60% (v/v) methanol. Progress curves for the hydrolysis of benzylpenicillin by cobalt β-lactamase II in 60% (v/v) ethylene glycol at temperatures below −30 °C consisted of a transient followed by a steady-state phase. The amplitude of the transient implied a burst whose magnitude was greater than the concentration of enzyme, and the proposed mechanism comprises a branched pathway. The kinetics for the simplest variants of such pathways have been worked out, and the rate constants (and activation parameters) for the individual steps have been determined. The spectrum of the enzyme changed during turnover: when benzylpenicillin was added to cobalt β-lactamase II, there was a large increase in the cysteine–cobalt(II) charge-transfer absorbance at 333 nm. This increase occurred within the time of mixing, even at −50 °C. The subsequent decrease in A_{333} was characterized by a rate constant that had the same value as the "branching" rate constant of the branched-pathway mechanism. This step is believed to be a change in conformation of the enzyme–substrate complex. Single-turnover experiments utilized the change in A_{333}, and the results were consistent with pre-steady-state and steady-state experiments. When a single-turnover experiment at −48 °C was quenched with acid, the low molecular weight component of the intermediate was shown to be substrate. The mechanism advanced for the hydrolysis of benzylpenicillin by cobalt β-lactamase II involves two noncovalent enzyme–substrate complexes that have been characterized by their electronic absorption spectra. When manganese β-lactamase II was used, the same features (implying a branched pathway) were evident; these experiments were carried out at ordinary temperatures and did not utilize a cryosolvent. The hydrolysis of nitrocefin by zinc β-lactamase II has been studied concurrently in 60% (v/v) methanol. Progress curves were triphasic. There were two transients preceding the linear steady-state phase. The stoichiometry of the burst again implied a branched pathway. The kinetics for a mechanism in which there are three intermediates (two of them lying in the branch) have been worked out and used to obtain values (and activation parameters) for four of the rate constants. Single-turnover experiments confirmed the kinetic scheme. An intermediate was detected spectroscopically; its calculated absorption spectrum resembled that of the substrate shifted to longer wavelengths. Low-temperature chromatography, carried out at varying intervals of time, revealed a second intermediate, accumulating at the expected rate. Acid-quench experiments suggested that all three intermediates were noncovalent enzyme–substrate complexes. The observation of pre-steady-state kinetics requiring a branched catalytic pathway for the zinc, manganese(II), and cobalt(II) forms of β-lactamase II provides convincing evidence for the proposed kinetic model. Branched pathways that comprise conformationally distinct complexes may be a consequence of protein fluctuations.

Characterizing intermediates is one of the main aims of those studying enzyme mechanisms. The use of low temperatures greatly extends the possibilities of characterizing intermediates (Douzou, 1977), particularly when spectroscopic methods are used; the power of this approach is exemplified by recent work on carboxypeptidase A (Auld et al., 1984). Chromophoric atoms or groups can be introduced into either the enzyme or the substrate, both being used in the present investigation.

β-Lactamases are mechanistically interesting and clinically important bacterial enzymes, some of which play an important part in the resistance of pathogens to β-lactam antibiotics. β-Lactamase II from *Bacillus cereus* (Sabath & Abraham, 1966) is distinguished by its requirement for metal ions such as Zn(II) or Co(II) for activity; it is also remarkably unselective and catalyzes the hydrolysis of a wide variety of β-lactams (Davies & Abraham, 1974; Abraham & Waley, 1979). Mechanistic studies on β-lactamase II have been previously concentrated on the groups that bind the metal ion (Baldwin et al., 1979, 1980a,b; Hill et al., 1980). β-Lactamase II is unaffected by the usual β-lactamase inhibitors, which are themselves β-lactams; β-lactamase II simply catalyzes their hydrolysis. The only other β-lactamase known to require metal ions for activity, the L1 enzyme from *Pseudomonas maltophilia* (Saino et al., 1982), appears to differ appreciably from β-lactamase II (Bicknell et al., 1985).

The choice of a suitable medium in cryoenzymology demands considerable study of catalysis in mixed aqueous–organic solvents, over a wide range of temperatures. This paper describes catalysis by β-lactamase II in cryosolvents including a detailed study of the hydrolysis of nitrocefin (I) (O'Callaghan et al., 1972) by zinc β-lactamase II and benzylpenicillin (II)

† Supported in part by the Medical Research Council and the E. P. Abraham Research Fund. This paper is a contribution from the Oxford Enzyme Group.

‡ Present address: Center for Biochemical and Biophysical Sciences and Medicine, Harvard Medical School, Brigham and Women's Hospital, Boston, MA 02115.

0006-2960/85/0424-6876$01.50/0

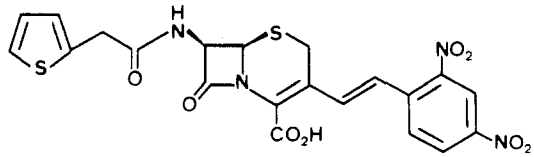

I

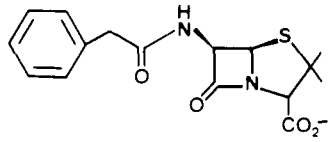

II

by cobalt β-lactamase II. Nitrocefin has the highest specificity constant known for zinc β-lactamase II (10^7 M^{-1} s^{-1}), has an exceptionally low K_m (1.65 μM), and shows large changes in absorbance on hydrolysis. Cobalt β-lactamase II has the great advantage of a "built-in" probe, and the favorable spectroscopic properties of the cobalt (II) have been utilized; for example, the absorption spectrum of the cobalt (II) enzyme is responsive to substrate binding, and this paper exploits this finding. Pre-steady-state and single-turnover experiments have been carried out at low temperatures, as well as steady-state experiments. These showed that branched-pathway mechanisms were operative for the zinc, cobalt(II), and manganese(II) forms of the enzyme. Two intermediates were characterized in the hydrolysis of benzylpenicillin by cobalt β-lactamase II and three intermediates, two lying in the branch, in the hydrolysis of nitrocefin by zinc β-lactamase II. The use of pre-steady-state kinetics at low temperatures also permitted determination of rate constants and activation parameters for individual steps in the proposed models.

Materials and Methods

Materials

β-Lactamase II from *Bacillus cereus* 569/H/9 was prepared as described previously (Davies et al., 1974; Baldwin et al., 1980b) as was the apoenzyme of β-lactamase II (Bicknell et al., 1983) with the one exception that 10 mM rather than 100 mM succinate buffers were employed. Cobalt β-lactamase II was prepared from the apoenzyme and aqueous $CoCl_2$ immediately before the experiment.

Nitrocefin (O'Callaghan et al., 1972) (I) was from Becton Dickinson UK Ltd., Oxford, U.K. Benzylpenicillin (II) was a gift from Glaxo Laboratories, Greenford, Middx, U.K. The α-methyl ester (III) of nitrocefin was prepared by heating

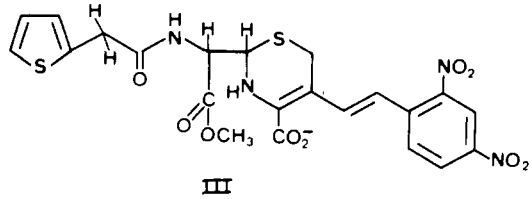

III

nitrocefin (2 mg) in dried methanol (10 mL) under reflux for 7 h. The reaction was then judged to have gone to completion by the observation of only a single spot by TLC (thin-layer chromatography) analysis [R_f 0.478 (red), nitrocefin R_f 0.17 (yellow), hydrolyzed nitrocefin R_f 0.054 (red)]. TLC was performed on DC-Plastikfolien Kieselgel 30 F_{254} plates in chloroform–acetone–acetic acid (55:45:5). The methyl ester showed λ_{max} 482.5 nm (100 mM succinate, pH 6.0) and a shoulder at 310 nm. ^1H NMR ($CDCl_3$) was expected with a single methoxy resonance at δ 3.85 (s). ^1H NMR spectra were recorded on a Bruker WH 300 Fourier-transform spectrometer with quadrature detection.

Methanol was Aristar grade from British Drug Houses. Ethylene glycol was from Fluka Ltd., puriss p.a. grade.

Methods

Solvents containing buffers were prepared as described by Douzou et al. (1976). The composition of solvents was by volume, and so v/v is omitted throughout for brevity. The apparent protonic activity (pH*) in the aqueous–organic solvent was the reading on a glass electrode at 0 °C for buffers required at this temperature—see also Douzou et al. (1976). Stock solutions of nitrocefin (5 mM) were prepared by dissolving nitrocefin (2.58 mg) in dimethylformamide (50 μL) followed by the addition of methanol (550 μL) and aqueous buffer (400 μL of 20 mM sodium cacodylate containing 0.4 mM zinc sulfate, pH 5.0). β-Lactamase II concentrations were determined on the basis of A_{280} = 1 for a 45.45 μM solution. Stock solutions of zinc β-lactamase II were prepared by dissolving freeze-dried enzyme in the aqueous component of the respective cryobuffer at 0 °C. There showed no loss in activity on being kept at 4 °C. For assays at subzero temperatures, the cosolvent was added to the stock enzyme solution, immediately before use, after being cooled to <2 °C. The enzyme was insufficiently soluble in aqueous methanol to obtain concentrated stock solutions, and so a ternary mixture of ethylene glycol–MeOH–H_2O (50:25:25) (by volume) was used. Free energies of transfer were determined as described by Maurel (1978).

Determination of the Steady-State Kinetic Parameters. Progress curves for the hydrolysis of β-lactams were measured with a Cary 219 spectrophotometer. Specially constructed cell blocks that gave a large metallic surface area in contact with the cell walls were employed. The cell blocks were completely insulated externally with Armaflex. The cell faces were flushed with dry nitrogen. The cell blocks were themselves isolated by quartz windows from separate chambers consisting of insulation tubing in which the beam traveled. These were independently flushed with dry nitrogen. The area around the cell blocks contained silica gel to maintain a dry atmosphere; this area was, in addition, slowly flushed by the escaping dry nitrogen.

Mixing was achieved by the use of an automatic toothbrush with paddle attachment; 3-mL cells were used because of the greater ease of mixing. It is important to add the enzyme slowly to the cooled reaction mixture, with careful stirring, usually over a period of 2–5 min at the lower temperatures. When the above procedure was followed, controls in which either substrate or enzyme was added to solvent showed no detectable absorbance changes at any wavelength arising from inadequate mixing.

Temperatures were maintained at ±0.2 °C with a Neslab, Endocal ULT 80 cryostat. The cell temperature was monitored with a BAT-12 thermocouple.

The change in absorbance on hydrolysis was measured for each set of conditions of pH, solvent, and temperature. Rates were never found to be limited by the concentration of metal ion, and product inhibition was not detected. Progress curves were analyzed by the half-time method (Wharton & Szawelski, 1982); linearity of the plots and Selwyn's (1965) test were the criteria for simple Michaelis–Menten kinetics. A median program (Cornish-Bowden & Eisenthal, 1978) and a program that performed the complete $t_{1/2}$ analysis directly from the observed and final absorbances were used.

The hydrolysis of benzylpenicillin in 60% (v/v) ethylene glycol in sodium cacodylate, pH* 6.4, was measured by the change in A_{245}, which varied with temperature; the extinction

coefficient [$\Delta\epsilon$ (mM^{-1} cm^{-1})] was given by

$$\Delta\epsilon = mT + 0.248$$

where $m = 1.739$ and T is the temperature (°C).

The change in A_{568} on hydrolysis of nitrocefin in 60% (v/v) methanol–40 mM sodium cacodylate, pH* 6, containing 0.4 mM $ZnCl_2$ also varied with the temperature, $\Delta\epsilon$ (mM^{-1} cm^{-1}) being given by $\Delta\epsilon = mT + 9.776$, where $m = 2.72 \times 10^{-2}$ and T is the temperature (°C).

Analysis of Progress Curves. Biphasic progress curves were fitted to eq 1, where p is the concentration of product at time

$$p = Vt + B(1 - e^{-Rt}) \quad (1)$$

t, R is the observed first-order rate constant characterizing the transient, B is the burst, and V is the final (steady-state) rate. Direct fitting of data to eq 1 by nonlinear regression utilized the fact that the parameters V and B appear as linear terms and so a normal equation is readily obtained with only one unknown, R. The nonlinear equation for R was solved by the bisection method. An improved (differential) method was used to avoid interference from the small amount of product (no more than 3% of the burst) formed as the temperature rises during mixing after addition of the enzyme. After the temperature had returned to the original value (about 5 min), successive points on the progress curve were taken at times separated by a constant time interval, Δt. If the concentrations of product at times t and $t + \Delta t$ are p and p', then

$$p' - p - V\Delta t = B(1 - e^{-R\Delta t})e^{-Rt}$$

and a plot of ln ($p' - p - V\Delta t$) against t will be linear; V was determined as the slope of the linear (steady-state) part of the progress curve. The reliability of this procedure was confirmed by simulations that introduced the measured rise in temperature during mixing.

Low-Temperature Exclusion Chromatography. An all-glass, jacketed column (1 cm^2 × 50 cm) was used for low-temperature gel filtration. The temperature of the column was maintained to within ±0.2 °C by the rapid circulation of ethanol from a Neslab, ULT 80, ultralow-temperature cryostat. The glass jacket was externally insulated with Armaflex. The time taken for the elution of the void volume for a 6 × 1 cm column of Sephadex LH-20 in the −50 to −70 °C temperature range was about 40 min.

Reactions were initiated on top of the resin by adding substrate (in cryobuffer) to the precooled enzyme solution. Stirring was carried out manually with a thin glass rod. After incubation for the required time, the reaction mixture was run into the resin, followed by an equal volume of buffer. The column was then filled with elution buffer and left to run. Fractions were collected at room temperature.

RESULTS

Choice of Cosolvents and Substrates. The first step in investigating conditions that might be suitable for low-temperature catalysis is to test whether the enzyme is stable in a given solvent mixture. Catalytic power, usually the most sensitive property of an enzyme, was examined. Zinc β-lactamase II was kept (for 24 h) at pH* 6, 4 °C, in 70% methanol, 65% dimethyl sulfoxide, or 50% dimethylformamide: there was no loss of enzymic activity. Solvents containing methanol were less viscous and were preferred. Different conditions had to be found for cobalt β-lactamase II, which was not stable in 50% dimethyl formamide or in 50% methanol but was stable in 65% dimethylsulfoxide, 60% ethylene glycol, or 40:40:20 ethylene glycol–water–methanol. The stability of the enzyme during catalysis was checked by Selwyn's (1965) test, particularly necessary for β-lactamases, which are prone to lose activity during turnover; e.g., zinc β-lactamase II was stable in 70% methanol, but Selwyn's test showed inactivation during the hydrolysis of nitrocefin in 70% methanol but not at 60% methanol. All the experiments to be described were carried out under conditions where Selwyn's (1965) test had shown the enzyme to be stable during turnover.

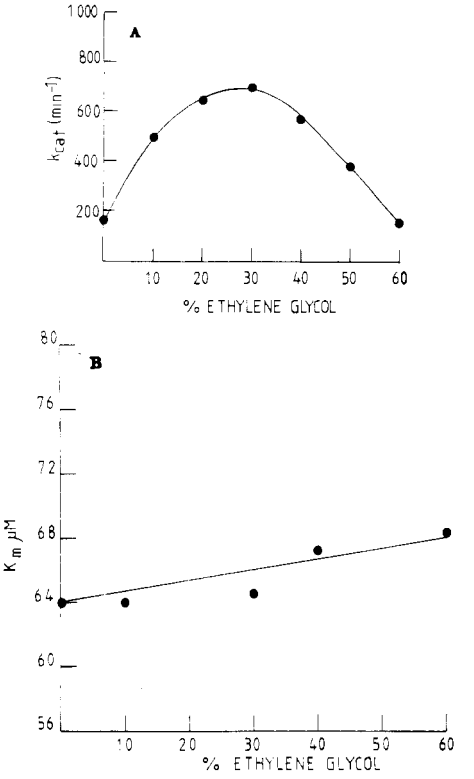

FIGURE 1: Effect of cosolvent on the kinetic parameters for hydrolysis of benzylpenicillin by cobalt β-lactamase II in aqueous ethylene glycol (0.08 M sodium cacodylate, 1 mM Co^{2+}, pH * 6.4, 0.4 °C).

Effects of Cosolvent on Steady-State Kinetics. The effects of cosolvent on kinetics were investigated by varying the concentration of cosolvent at 0 °C, so that direct comparison with aqueous controls could be made. The cosolvents chosen did not have a deleterious effect on catalysis: in fact, as will be described, the presence of cosolvent sometimes increased k_{cat}. The often large increase in K_m in the presence of cryosolvent has the important practical disadvantage that high concentrations or reactants have to be used to attain high concentrations of complex. Thus, systems were sought in which (a) the enzyme was soluble and stable during catalysis, (b) the course of the reaction could be analyzed spectrophotometrically, and (c) the K_m was as low as possible.

Hydrolysis of benzylpenicillin (II) by cobalt β-lactamase II in ethylene glycol had the advantage that K_m was low; here, k_{cat} first increased and then decreased (Figure 1), but K_m was largely unchanged. A similar dependence was seen with cobalt β-lactamase II and several other penicillins (data not shown). Thus, although water is a reactant, solvent effects are dominant, and the molecularity with respect to water cannot be measured from experiments in mixed solvents. A maximum for k_{cat} at intermediate concentrations of cosolvent has been reported for several enzymes and ascribed to enhanced flexibility of the protein (Tan & Lovrien, 1972; Dreyfus et al., 1978). With zinc β-lactamase II and nitrocefin, k_{cat} increased with the concentration of cosolvent, for both methanol and dimethyl sulfoxide, as did K_m (Figure 2). Maurel (1978) has shown that for several enzymes the increase in K_m that follows the introduction of cosolvent may be correlated with the in-

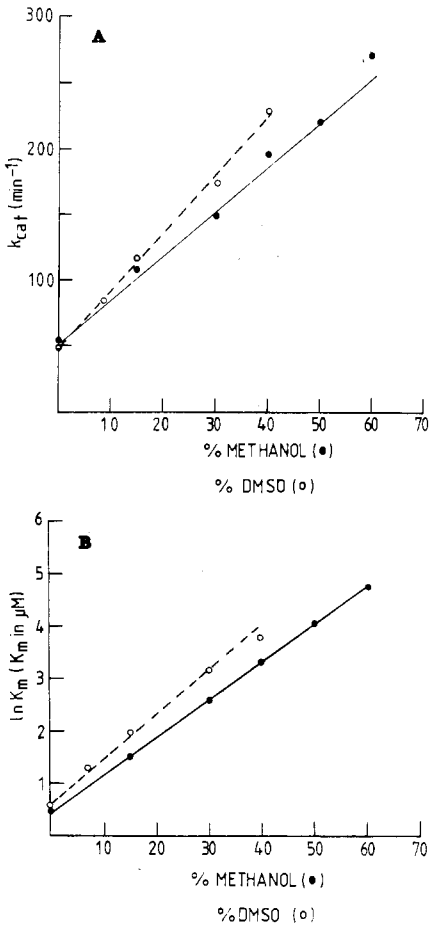

FIGURE 2: Effect of cosolvent on k_{cat} and K_m for hydrolysis of nitrocefin by zinc β-lactamase II. Cryosolvent was methanol, pH* 6 (●), or dimethyl sulfoxide, pH* 7 (○), 0.05 M sodium cacodylate, 0.05 M NaCl, and 0.4 mM Zn^{2+}, 0.4 °C.

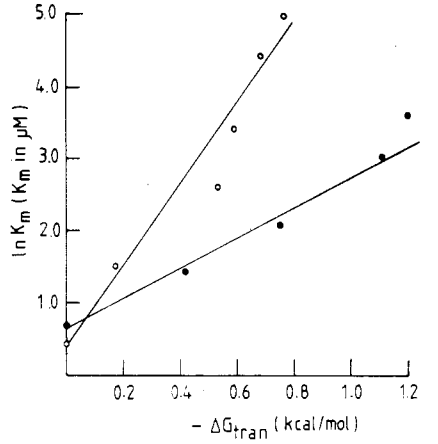

FIGURE 3: Plot of ln K_m(app) against ΔG transfer for the hydrolysis of nitrocefin by zinc β-lactamase II in methanol–water (○) and dimethyl sulfoxide–water (●) mixtures, where ΔG transfer = $-RT$ ln (solubility in cryosolvent/solubility in water).

creased solubility of the substrate in the organic/aqueous media relative to that in water. The relative solubility was expressed as the free energy transfer of the substrate between the cryosolvent and water. No relationship between the dielectric constant and K_m was found (Maurel, 1978). The same was true for zinc β-lactamase II and nitrocefin. Thus, although addition of dimethyl sulfoxide to water does not change the dielectric constant, whereas methanol gives rise to a marked decrease (Douzou et al., 1977), both solvents caused very similar changes in the kinetic parameters. In contrast, Figure

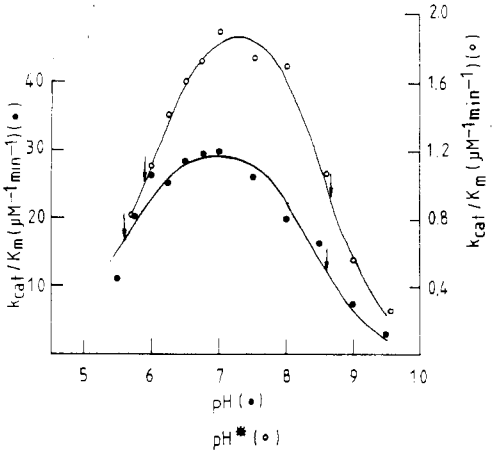

FIGURE 4: pH dependence of k_{cat}/K_m for hydrolysis of nitrocefin by zinc β-lactamase II in water (●) and 60% methanol (○) at 0.4 °C in 0.05 M NaCl. The buffers in water were as follows: pH 5.5–6.25, 0.02 M sodium succinate, 1 mM Zn^{2+}; pH 6.5–8, 0.02 M 4-morpholinepropanesulfonic acid, 0.1 mM Zn^{2+}; pH 8.5–9.5, 0.02 M sodium borate, 0.05 mM Zn^{2+}. The buffers in 60% methanol were as follows: pH* 5.75–6, 0.05 M sodium acetate, 1 mM Zn^{2+}; pH* 6.5–8, 0.05 M sodium cacodylate, 0.1 mM Zn^{2+}; pH* 8.5–10, 0.05 M Tris, 0.01 mM Zn^{2+}.

Table I: Apparent Energies of Activation for Steady-State Kinetic Parameters for β-Lactamase II in Water Cryosolvents[a]

solvent	substrate	energy of activation at 0 °C (kcal/mol) k_{cat}	k_{cat}/K_m	K_m
	Zinc β-Lactamase II			
water	nitrocefin	17.5		
60% methanol	nitrocefin	17	17.5	0.58
water	benzylpenicillin	15.3		
50% methanol	benzylpenicillin	17.5	13.5	0.39
	Cobalt β-Lactamase II			
water	benzylpenicillin	21.2		
60% ethylene glycol	benzylpenicillin	20	19.4	0.76

[a] The hydrolysis of benzylpenicillin was measured in the pH-stat over 0–30 °C; the initial substrate concentration was at least 30 K_m when k_{cat} was being determined. The hydrolysis of nitrocefin was measured at 568 nm.

3 shows that the increase in K_m correlates well with ΔG transfer for nitrocefin in both solvents. We conclude that the cosolvent effect on K_m is simply a weakening of binding, a result of the increased solubility of nitrocefin in the organic/aqueous solvents. The pH dependence of k_{cat}/K_m was strikingly similar in water and 60% methanol at 0 °C (Figure 4), in spite of the difference in the absolute values of the parameter between the two solvents. The pH dependence of k_{cat} was less informative because k_{cat} only decreased at pH values where the enzyme was unstable (data not shown). The possibility that the increase in k_{cat} for nitrocefin in aqueous methanol could arise from methanolysis was examined. However, none of the α-methyl ester was detected on TLC of the reaction mixture, nor was the α-methyl ester hydrolyzed by the enzyme. Knott-Hunziker et al. (1982) noted that zinc β-lactamase II did not catalyze the methanolysis of benzylpenicillin, nor was there acyl transfer with depsipeptides (Pratt & Govardhan, 1984). No nucleophile has yet been found to replace water in the action of β-lactamase II. There were no discontinuities in Arrhenius plots (Figures 6 and 10), and the apparent energies of activation (at 0 °C) in water and cryosolvents were similar (Table I). This similarity is the usual criterion for believing that the mechanism is not fundamentally different in the presence of cryosolvent at low temperatures.

Table II: Kinetic Parameters and Rate Constants for Branched Mechanisms[a]

parameter	mechanism I	mechanism II
V	$k_4(k_2 + k_3)e_0/(k_3 + k_4)$	$k_2k_4e_0/(k_3 + k_4)$
B	$k_3(k_2 - k_4)e_0/(k_3 + k_4)^2$	$k_2k_3e_0/(k_3 + k_4)^2$
R	$k_3 + k_4$	$k_3 + k_4$
k_{cat}	$(k_2 + k_3)k_4/(k_3 + k_4)$	$k_2k_4/(k_3 + k_4)$
k_{cat}/K_m[b]	$(k_2 + k_3)/K_s$	k_2/K_s
K_m[b]	$K_sk_4/(k_3 + k_4)$	$K_sk_4/(k_3 + k_4)$

[a] The mechanisms are given in the text. [b] The approximation $k_1 \gg k_2$ and k_3 is used and is justified in the text.

Cobalt β-Lactamase II: Progress Curves and the Size of the "Burst". The hydrolysis of benzylpenicillin by cobalt β-lactamase II was sufficiently slow at temperatures below −30 °C (in 60% v/v ethylene glycol) to observe the approach to the steady state. When the concentration of substrate far exceeded K_m, there was an exponential pre-steady-state (transient) phase followed by a linear steady-state phase. The transient phase lasted for at least 0.5 h. The transient phase was not caused by interconversion of different forms of the enzyme: when the enzyme was kept at −29 °C for 4 h before adding substrate, the progress curve was indistinguishable from that obtained by adding enzyme to substrate. Thus, the transient was a "substrate-induced" effect. The concentration of Co(II) over the range 0.1–100 mM did not affect the rate of hydrolysis. There was no detectable nonenzymic hydrolysis of benzylpenicillin in the presence of Co(II) at subzero temperatures.

When the linear (steady-state) part of a progress curve was extrapolated back, the intercept on the ordinate gave the burst. A significant feature of the present experiments was that the burst was about 80 times the concentration of the enzyme. Now a burst that is greater than the concentration of the enzyme, in a reaction in which there is only one product (which is not an inhibitor), entails a branched-pathway mechanism (Charnas & Knowles, 1981). Thus, there must be two species, ES^1 and ES^2, and the simplest mechanisms are

mechanism I

$$E + S \underset{}{\overset{K_s}{\rightleftharpoons}} ES^1 \xrightarrow{k_2} E + P$$
$$\Big\downarrow k_3$$
$$ES^2 \xrightarrow{k_4} E + P$$

mechanism II

$$E + S \underset{}{\overset{K_s}{\rightleftharpoons}} ES^1 \xrightarrow{k_2} E + P$$
$$k_4 \Big\uparrow\Big\downarrow k_3$$
$$ES^2$$

These mechanisms differ in that ES^2 is active in I but not II. The transient-phase kinetics for both mechanisms have been solved, and the three rate constants (and the dissociation constant for substrate binding) may be obtained. Progress curves were fitted to eq 1; the analysis assumed (a) that the enzyme was saturated throughout the transient, which was shown by the zero-order kinetics after the transient had finished, (b) that the complex ES^1 was in equilibrium with E, which was confirmed experimentally (see later), and (c) that the steps with rate constants k_2 and k_4 in I or k_2 in II were those that gave rise to the observed change in A_{245} due to opening the β-lactam ring.

When $s_0 \gg K_m$ and $s_0 \gg e_0$, where the concentrations of substrate and enzyme are s_0 and e_0, then use of the Laplace–Carson transformation [see, e.g., Rodiguin & Rodiguina (1964)] yields solutions for progress curves for mechanisms I and II of the form of eq 1 with the parameters having the values given in Table II. The rate constants were found from the parameters V, B, and R as follows. First, $k_2 = (V + RB)/e_0$ and $k_3 = R - k_4$, whence, for mechanism I, $k_4^2 - (k_2 + R)k_4 + RV/e_0 = 0$ permits evaluation of k_4. For mechanism II, $k_4 = RV/(k_2e_0)$. It turned out that either mechanism I or II could account for the findings, and both (within the experimental error) gave the same values for the rate constants. The Arrhenius plot for the rate constants (Figure 5) gave the parameters in Table III. The second entry differs appreciably from the other two, and this is consistent with the view that the step associated with k_3 is a conformational change. Further evidence was provided by the experiments in which the UV absorbance of the enzyme was measured, described in the next section.

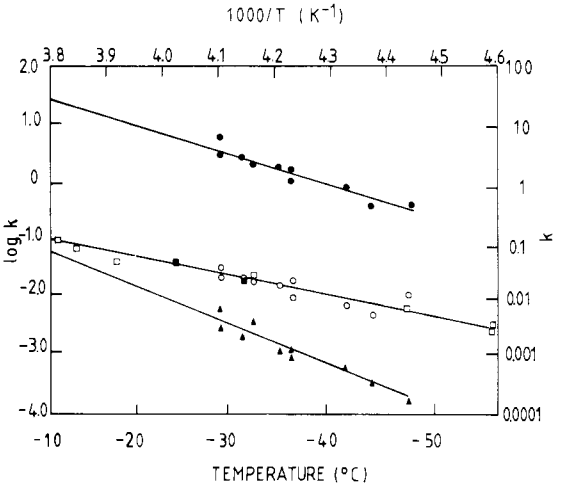

FIGURE 5: Arrhenius plot of rate constants for branched-pathway mechanism for the hydrolysis of benzylpenicillin by cobalt β-lactamase II in 60% ethylene glycol at pH* 6.4. Results from the change in A_{245} (due to opening the β-lactam ring): k_2 (●); k_3 (○); k_4 (▲). The lines are least-square fits of the linear form of the Arrhenius equation. Results from the change in A_{343} (due to cobalt charge-transfer interaction) (□) and from the change in fluorescence intensity at 328 nm, with excitation at 280 nm (■).

Table III: Parameters from Arrhenius Plots of Rate Constants for the Hydrolysis of Benzylpenicillin by Cobalt β-Lactamase II[a] and Manganese β-Lactamase II[b]

	E (kcal/mol)		A (min^{-1})	
rate constant	Co(II)	Mn(II)	Co(II)	Mn(II)
k_2	14.0	20.4	1.52×10^{13}	3.25×10^{18}
k_3	8.18	10.9	5.7×10^{5}	1.95×10^{11}
k_4	17.8	10.9	5.0×10^{13}	1.57×10^{6}

[a] Benzylpenicillin and Cobalt(II) β-lactamase II in 60% (v/v) ethylene glycol at pH* 6.4. [b] Benzylpenicillin and Manganese(II) β-lactamase II in 1 mM $MnCl_2$ and 0.5 M NaCl, pH 6 (pH-stat assays).

Two tests of the adequacy of the models and procedures were carried out. Theoretical progress curves were generated with the program KINSIM of Barshop et al. (1983) and found to give satisfactory agreement with points obtained experimentally. The second test was to see whether the values in Table III [effectively, $k_3k_5/(k_4 + k_5)$ as $k_3 \gg k_4$] gave values for k_{cat} at higher temperatures (i.e., −25 to 0 °C) that agreed with those found. This was so (Figure 6). It may also be seen that the temperature-dependence of k_{cat} in cryosolvent (60% ethylene glycol) and water was similar.

Spectral Changes in Cobalt β-Lactamase II during Turnover. The UV spectrum of cobalt β-lactamase II in 60% ethylene glycol at −48 °C had λ_{max} 343.3 nm and ϵ_M 878, at

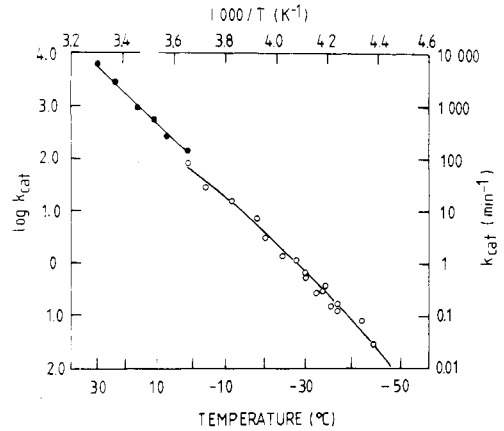

FIGURE 6: Arrhenius plot of k_{cat} for hydrolysis of benzylpenicillin by cobalt β-lactamase II in water (●) (pH 6.4) and in 60% ethylene glycol (○) (pH* 6.4). The line for the points in water is a least-squares fit, and the line for the points in cryosolvent is calculated from the expression in Table II for k_{cat} for model I (the line for model II does not differ significantly).

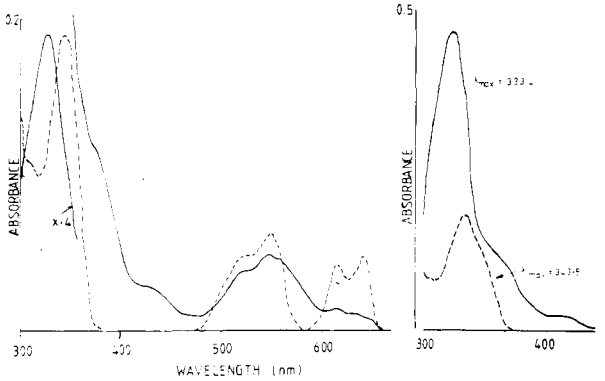

FIGURE 7: Absorption spectra of 0.133 mM cobalt β-lactamase II in 60% ethylene glycol at −48 °C (80 mM sodium cacodylate, 1 mM cobalt chloride, pH* 6.4) before (−−) and 5 min after the addition of 20 mM benzylpenicillin. The pathlength was 1 cm, and the reference cell contained 1 mM cobalt chloride; the inset shows absorbance 0–0.5.

pH* 6.4, little different from the values at 30 °C (λ_{max} 348 nm, ϵ_M 864; Baldwin et al., 1980). When benzylpenicillin was added at −48 °C (to a concentration of $7K_m$), the absorbance increased immediately: the new peak had λ_{max} 333.4 nm and ϵ_M 6200 (Figure 7). This peak then slowly decayed. Significantly, the first-order progress curve gave a rate constant indistinguishable from k_3, over a range of temperature (Figure 5). The same process could be monitored by the increase in fluorescence, excitation being at 280 nm. The fall in A_{343} after the initial very rapid increase is given by eq 2, where ϵ_x and

$$\Delta A = (\epsilon_y - \epsilon_x)\frac{k_3 e_0}{k_3 + k_4}[1 - e^{-(k_3 + k_4)t}] \qquad (2)$$

ϵ_y are the molar extinction coefficients of ES^1 and ES^2, respectively; the concentration of free enzyme in these experiments was negligible since increasing the initial concentration of substrate did not alter the progress curves. Both mechanisms give eq 2. The absorbance when $t \gg (k_3 + k_4)^{-1}$ approached $\epsilon_y e_0$ as virtually all of the enzyme was present as ES^2. Since $k_3 \gg k_4$ over this range of temperatures, these results are consistent with eq 2, and the new peak may be assigned to ES^1. The new peak was formed within the time of mixing even at −65 °C; this shows that substrate binding is a rapid equilibrium process. After the peak assigned to ES^1 had decayed, the spectrum (due to ES^2) had λ_{max} 343.3 nm as in the free enzyme, but ϵ_M was 415 rather than 878. Reliable kinetic data for the slow last phase, $ES^2 \rightarrow E$, was not obtained.

Table IV: Acid Quench of β-Lactamase II and Benzylpenicillin[a]

compound	R_f	radioactivity (cpm) i	ii
benzylpenicillin	0.57	43 238	42 719
benzylpenicilloate	0.22	703	528

[a] Radioactive penicillin [potassium 6-(phenyl[1-^{14}C]acetamido)-penicillanate] (final concentration 0.5 mM) was added to 1.6 mM cobalt β-lactamase II at −53 °C in 60% (v/v) ethylene glycol; virtually all of the substrate was enzyme-bound. The increase in A_{333} showed the formation of ES^1 (see text; about 30% of the enzyme was as ES^1). Then (within 40 s) 60 μL of 0.4 M HCl in 60% (v/v) ethylene glycol was added to give a pH* of 3; A_{333} promptly decreased again. The mixture was analyzed by TLC in acetone–acetic acid (19:1 v/v) on DC-Plastikfolien Kieselgel 30 F_{254} plates, and the compounds were estimated by scintillation counting. The results of two experiments are given.

Completion of consumption of substrate could be hastened by warming to 0 °C; cooling to −48 °C then gave the spectrum of free enzyme. Addition of a second portion of benzylpenicillin restored the peak assigned to ES^1: the entire sequence could then be repeated. This confirmed that there were no irreversible changes.

Cobalt β-Lactamase II: Single Turnover Experiments. When the concentration of the enzyme was greater than the initial concentration of substrate, there was an exponential decrease in A_{333}; experiments were carried out at both −30 and −53 °C, and the concentration of enzyme was varied over the range 20–220 μM, the concentration of benzylpenicillin being 2–5 μM. The observed first-order rate constant was directly proportional to the concentration of enzyme; at −30 °C the slope gave k_2/K_s = 2.7 mM^{-1} min^{-1}, in fair agreement with the steady-state value of k_{cat}/K_m (3.87 mM^{-1} min^{-1}); at −53 °C, k_2/K_2 = 0.316 mM^{-1} min^{-1}. Consistency between single-turnover and steady-state experiments is an important test of kinetic mechanisms. A single-turnover experiment was quenched with acid, in the experiment now described.

Nature of the Low Molecular Weight Component of ES^1. The formation of ES^1 from radioactive benzylpenicillin and excess cobalt β-lactamase II in 60% ethylene glycol at −48 °C was monitored by the increase in A_{333}. The reaction was quickly stopped with acid; nearly all (88%) of the low molecular weight material was benzylpenicillin (i.e., substrate) (Table IV). The remainder was product, and about 10% of product would be expected from the value of k_2. Thus, ES^1 must presumably be an enzyme–substrate noncovalent complex. For if it were a labile covalent complex, e.g., a mixed anhydride or an acylimidazole, decomposition would yield benzylpenicilloic acid.

Cobalt β-Lactamase II: Low-Temperature Exclusion Chromatography. One of the advantages of cryoenzymology lies in the possibility of isolating intermediates. The cryosolvent was changed to water–ethylene glycol–methanol (40:40:20, by volume) as 60% ethylene glycol was too viscous for chromatography at −48 °C. The change of cryosolvent had only a minor effect on the kinetics (data not shown). Radioactive benzylpenicillin (4 mM) and cobalt β-lactamase II (20 μM) were either submitted directly to exclusion chromatography or kept for 18 h at −48 °C for the transient to finish before chromatography on Sephadex LH-20 at −48 °C. In the first case, there was no radioactivity associated with the protein peak in the fractions containing protein, whereas in the second case there was one molar portion of radioactivity. The calculated half-lives of ES^1 and ES^2 at −48 °C were 1.9 and 3500 min, respectively, and the chromatography took 40 min. The

results thus confirmed that ES^1 was too labile to isolate but that ES^2 could be isolated. The nature of ES^2 is uncertain; after warming to room temperature, benzylpenicilloic acid was present. The mechanisms advanced are consistent with ES^2 being a second noncovalent enzyme–substrate complex. This view was supported by chromatography at −48 °C after treatment of reaction mixture with acid: there was no radioactivity associated with the protein.

Hydrolysis of Benzylpenicillin by Manganese β-Lactamase II. At ordinary temperatures, the hydrolysis of benzylpenicillin by manganese (II) β-lactamase II gave markedly biphasic progress curves. The initial rate at 30 °C was 8% that of the Zn(II) enzyme, as reported (Baldwin et al., 1980a). Again, the burst size was larger than the concentration of enzyme by a factor of the order of 10^4. The final rate was only 0.3% of that of the Zn(II) enzyme. After the transient had finished, zero-order kinetics were observed. Finally, after all the substrate had been consumed, full activity was recovered. Tests showed that the change in activity needed the presence of substrate and was not observed on incubation of the apoenzyme with benzylpenicillin (30 mM). Here activity was measured by discontinuous assay in which portions were diluted into a solution containing benzylpenicillin (and zinc) in the pH stat. Thus, the main features seen with cobalt β-lactamase II at subzero temperatures were observed with the Mn(II) enzyme at ordinary temperatures. The results of experiments over the range 10–40 °C were interpreted on the mechanisms described for cobalt(II) β-lactamase II. The values of the rate constants are given in Table III; k_2 is appreciably greater than k_3 or k_4. The largeness of the preexponential term for k_2 may be more apparent than real, a result of the long extrapolation required to estimate it.

Zinc β-Lactamase II: Triphasic Progress Curves. Low temperatures (below −47 °C) were required to study the pre-steady-state phase of the hydrolysis of nitrocefin by zinc β-lactamase II. The progress curves comprised two exponential phases and a (final) linear phase (Figure 8). The linear phase persisted over many hours; the initial substrate concentration was about $20K_m$, and no inhibition by product was detected. This confirms the stability of the enzyme in cryosolvent during turnover. Extrapolation of the linear part of the progress curve back to the ordinate enabled the burst to be found: the burst was 6 times greater than the concentration of enzyme (Figure 8). When the enzyme was kept at −61 °C for 4 h before adding substrate to start the reaction, the progress curve was indistinguishable from that found when the reaction was started by adding enzyme to chilled substrate. The size of the burst and the final rate were both directly proportional to the concentration of enzyme (data not shown). The size of the burst, as with cobalt β-lactamase II and benzylpenicillin, implied a branched pathway. The rates were independent of the concentration of zinc chloride over the range 0.1–10 mM.

The analysis of the triphasic curves is now described. Progress curves were fitted to eq 3 where p is the concentration

$$p = B + Vt + A_1e^{-a_1t} + A_2e^{-a_2t} \quad (3)$$

of product, V is the final rate, B is the burst, and the two transients are characterized by time constants a_1 and a_2 and amplitudes A_1 and A_2. The analysis started at the time which was, in effect, treated as the origin of the progress curve (about 3 min) by which the temperature had fallen to its original value. The vertical distance between the line and curve in Figure 8 is $B + Vt - p$. The plot of ln $(B + Vt - p)$ against time was linear at the longer times, when the first transient had been completed; the slope and intercept gave a_2 and A_2.

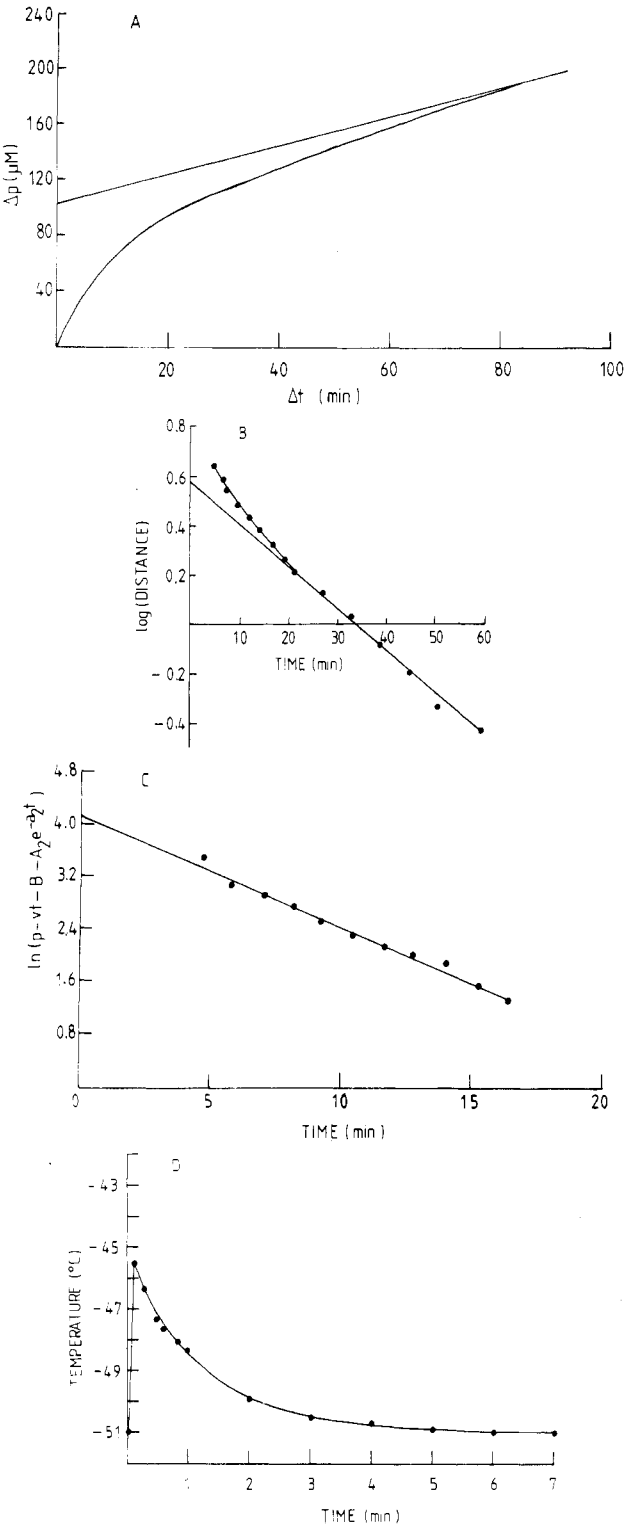

FIGURE 8: Hydrolysis of nitrocefin by zinc β-lactamase II at −51 °C. Nitrocefin (0.8 mM) and β-lactamase II (15 μM) were in 60% methanol containing 40 mM sodium cacodylate and 1 mM zinc chloride, pH* 6; A_{568} was measured as a function of time. (A) Triphasic progress curve; for concentration of product (origin shifted), see text. (B) Semilogarithmic plot of distance from curve to line. (C) Plot of ln $(1 - Vt + B - A_2e^{-a_2t})$ against time; the symbols are defined in the text. The found values for the transients were $A_1 = -65.4$ μM, $A_2 = -68.55$ μM, $a_1 = 0.243$ min^{-1}, and $a_2 = 0.036$ min^{-1} and for the rate constants were $k_2 = 1.46$ min^{-1}, $k_3 = 0.18$ min^{-1}, $k_4 = 0.076$ min^{-1}, and $k_s = 0.022$ min^{-1}. (D) Cell temperature as a function of time.

Then, a plot of ln $(B + Vt - p - A_2e^{-a_2t})$ against time was linear and gave a_1 and A_1 (Figure 8). The time constants at a given temperature were independent of the concentration of enzyme.

Table V: Relationship between Kinetic Parameters and Rate Constants

parameter	expression
V	αe_0
B	$e_0(\beta/a_1 + \gamma/a_2)$
A_1	$-(\beta/a_1)e_0$
A_2	$-(\gamma/a_2)e_0$
α	$k_4k_5(k_2 + k_3)/(k_3k_5 + k_4k_5 + k_3k_4)$
β	$(k_2k_3k_5 - k_2k_3a_1 + k_2k_3k_4 - k_3k_4k_5)/[a_1(a_2 - a_1)]$
γ	$(k_2k_3k_5 - k_2k_3a_2 + k_2k_3k_4 - k_3k_4k_5)/[a_2(a_1 - a_2)]$
$a_1 + a_2$	$k_3 + k_4 + k_5$
a_1a_2	$k_3k_5 + k_4k_5 + k_3k_4$
K_s	$K_m[1 + (k_3/k_4)(1 + k_4/k_5)]$

Table VI: Parameters from Arrhenius Plots of Rate Constants for the Hydrolysis of Nitrocefin by Zinc β-Lactamase II[a]

rate constant	E (kcal/mol)	A (min^{-1})
k_2	15.2	5.0×10^{14}
k_3	4.15	1.75×10^{3}
k_4	8.11	5.9×10^{6}
k_5	17.9	7.1×10^{15}

[a] In 60% (v/v) methanol containing 40 mM sodium cacodylate and 1 mM zinc chloride, pH* 6.

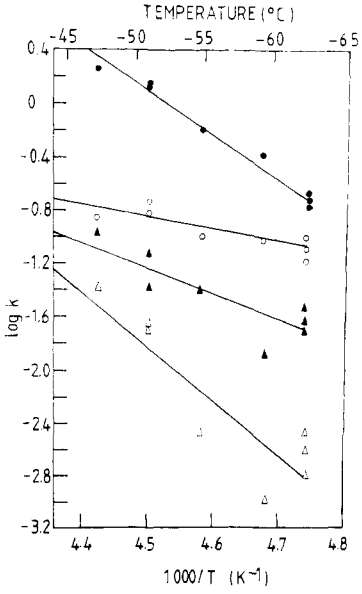

FIGURE 9: Arrhenius plot of rate constants for hydrolysis of nitrocefin by zinc β-lactamase II in 60% methanol: k_2 (●), k_3 (○), k_4 (▲), and k_5 (△).

The simplest kinetic mechanism that accounts for the facts is

$$E + S \underset{}{\overset{K_s}{\rightleftharpoons}} ES_1 \xrightarrow{k_2} E + P$$

$$\downarrow k_3$$

$$ES^2 \xrightarrow{k_4} ES^3 \xrightarrow{k_5} E + P$$

On the assumptions given above, eq 4 is of the same form as

$$p = e_0\left(\frac{\beta}{a_1} + \frac{\gamma}{a_2} + \alpha t - \frac{\beta}{a_1}e^{-a_1t} - \frac{\gamma}{a_2}e^{-a_2t}\right) \quad (4)$$

eq 3, and the relationships in Table V show how the measured parameters were used to obtain values for the rate constants. The initial rate gave an estimate of k_2, and eq 5 then gave k_3.

$$k_3 = (a_1\beta + a_2\gamma)/k_2 \quad (5)$$

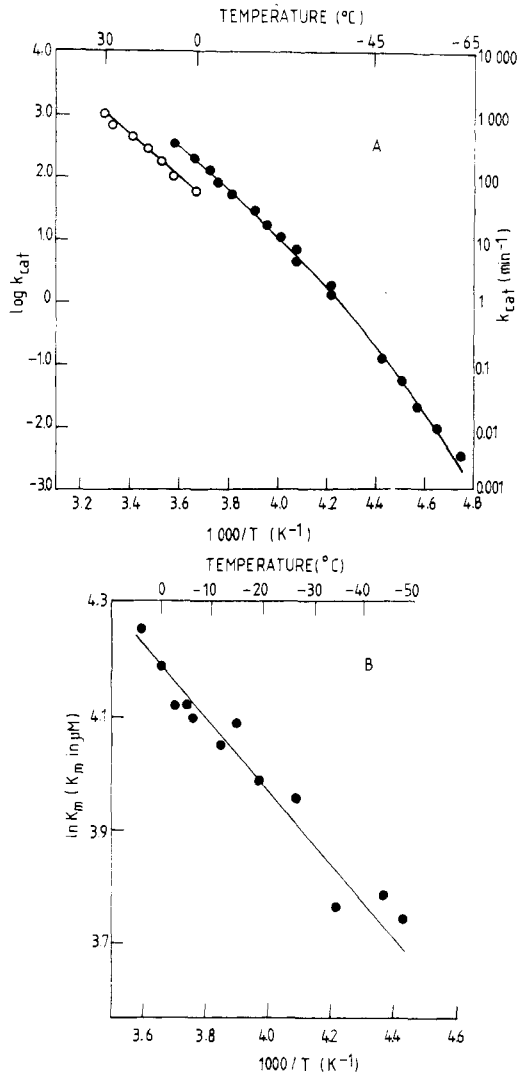

FIGURE 10: (A) Arrhenius plot of k_{cat} for hydrolysis of nitrocefin by zinc β-lactamase II in water (○) (pH 6) and in 60% methanol (●) (pH* 6). The line drawn through the points in water is a least-squares fit; that through the points in cryosolvent is calculated from the expression in Table V and the values in Table VI. (B) Effect of temperature on K_m for the hydrolysis of nitrocefin by zinc β-lactamase II in 60% methanol pH* 6).

Finally, the sum and product of the two remaining rate constants are given by eq 6 and 7; hence, it is not possible to say

$$k_4k_5 = a_1a_2\alpha/(k_2 + k_3) \quad (6)$$

$$k_4 + k_5 = a_1 + a_2 - k_4 \quad (7)$$

which is which. The exclusion chromatography however (see below), suggested that k_5 was less than k_4. The Arrhenius plots (Figure 9) gave the parameters listed in Table VI. Two of the four rate constants have particularly low values of both the apparent energies of activation (E_a) and the preexponential factor (A). The steady-state k_{cat} was calculated (given by α in Table V); the Arrhenius plot (Figure 10) was nonlinear, and the values calculated at less low temperatures (11 to −45 °C) agreed with those obtained experimentally. K_m showed a marked decrease with temperature (Figure 10).

Further information was provided by single-turnover experiments. Thus, at −42 °C the hydrolysis of nitrocefin by zinc β-lactamase II was slow enough to use concentrations of enzyme greater than those of the substrate. The kinetics were first order; the reaction here proceeds slowly by the "direct" pathway, since $k_2 \gg k_3$. The first-order rate constant was

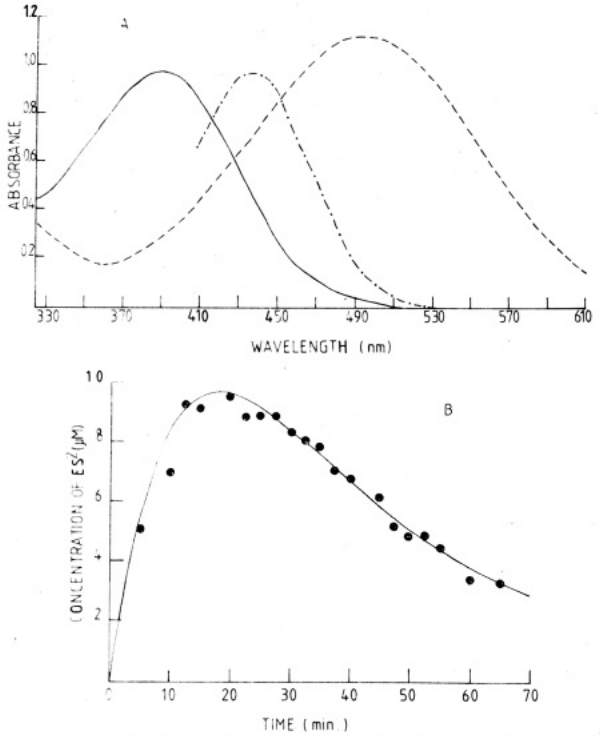

FIGURE 11: (A) Absorption spectrum calculated for nitrocefin intermediate (–·–) compared with those of substrate (—) and product (– –), measured in 60% methanol, pH* 6, –58.6 °C; the concentrations were 50 μM, and the path length was 1 cm. (B) The concentration of the intermediate as a function of time; the points were calculated from A_{450}, allowing for the contribution from product formed and correcting for depletion of substrate in the sample cell but not in the reference cell. The line was calculated with the rate constants given above, except that k_2 was 0.562 min^{-1}; the rise in temperature on mixing was probably not adequately allowed for, and so distorted the early part of the curve.

directly proportional to the concentration of enzyme (data not shown); the slope is k_2/K_s. From the value of k_2 (3.16 min^{-1} at –42 °C), K_s was 180 μM, in good agreement with the value of 155 μM calculated from the expression in Table V with the determined K_m of 43 μM.

Detection and Characterization of Intermediates in the Hydrolysis of Nitrocefin. In the experiments now to be described, difference spectra were recorded; the reference cell contained substrate but no enzyme. When the concentration of enzyme was greater than that of substrate, no intermediate was detected at –63 °C; the spectrum of ES^1 does not appear to differ appreciably from that of substrate. On the other hand, when the concentration of substrate was greater than that of enzyme, a shoulder at about 450 nm provided clear evidence of an intermediate. Low temperatures were essential; the shoulder was not observed at temperatures above –54 °C. The absorption spectrum of the intermediate was calculated by allowing for the contribution made by product and correcting for the depletion of substrate. When the absorbance at 600 nm was used to calculate the concentration of product, the excess absorption in the difference spectrum had become negligible at wavelengths beyond 540 nm. Hence, the contribution of product to the difference spectrum observed can be calculated from the absorbance at 600 nm. The correction to the calculated difference spectrum due to the depletion of substrate utilized the numerical integration procedure KINSIM (Barshop et al., 1983), knowledge of the individual rate constants, and K_s from the single-turnover experiments. The calculated absorption spectrum of the intermediate was found to resemble the substrate spectrum shifted to longer wavelength (Figure 11) and had λ_{max} 440 nm and ϵ 19 260 M^{-1} cm^{-1}. The

Table VII: Absorption Maxima for Nitrocefin and Derivatives

compound	solvent	λ_{max} (nm)
nitrocefin	H_2O, pH 6, 30 °C	386
	60% (v/v) methanol, pH* 6, –60 °C	392
	ethyl acetate	381
	ethanol	400
hydrolysis product of nitrocefin	H_2O, pH 6, 30 °C	491
	60% (v/v) methanol, pH* 6, –60 °C	491
α-methyl ester of nitrocefin	H_2O, pH 6, 30 °C	482.5
	60% (v/v) methanol, pH* 6, –60 °C	484.3
	ethyl acetate	485.7
	ethanol	496.3
dimethyl ester of nitrocefin	ethanol	447[a]
reaction intermediate[b]	60% (v/v) methanol, pH* 6, –60 °C	440

[a] O'Callaghan et al. (1972). [b] See text.

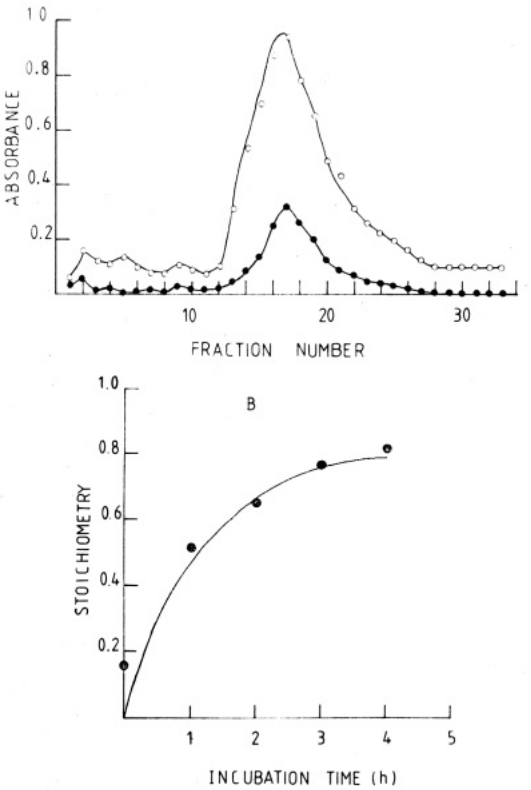

FIGURE 12: (A) Low-temperature chromatography on 6 × 1 cm^2 column of Sephadex LH-20 of reaction mixture of 0.18 mM nitrocefin, and 40 μM zinc β-lactamase II in 60% methanol, pH* 6, after being kept for 2 h at –64 °C: A_{280} (○); A_{500} (●). (B) Molar proportion of lower molecular weight material coeluting with protein as a function of time of reaction at –64 °C. Nitrocefin (0.18 mM) and zinc β-lactamase II (20 μM) in 60% methanol containing 40 mM sodium cacodylate, 40 mM NaCl, and 0.4 mM $ZnCl_2$, pH* 6. The theoretical curve drawn was for a first-order approach to 0.83 mol/mol, on the basis of an estimated K_m of 34 μM.

λ_{max} is compared with those of nitrocefin and related compounds in Table VII. The absorption of the intermediate was calculated as a function of time of reaction and compared with the calculated concentration of ES^2: the agreement was satisfactory (Figure 11).

Zinc β-Lactamase II: Low-Temperature Chromatography. After 2 h at –64 °C, a reaction mixture was analyzed by chromatography in Sephadex LH-20 at this temperature: there was a peak of both A_{280} and A_{500} emerging at tube 15 after about 1 h (Figure 12). This is ascribed to enzyme-bound nitrocefin (or a derivative thereof); in control experiments (lacking enzyme), both nitrocefin and its hydrolysis product were bound exceptionally tightly and were not eluted before

fraction 120. When the experiments was carried out at −45 °C instead of −64 °C, the early A_{500} peak was no longer present. The calculated half-lives of ES^1, ES^2, and ES^3 were 2.8, 47, and 870 min at −64 °C, and so ES_3 (and some ES^2) will be present after 1 h at −64 °C. At −45 °C, however, the intermediates are not stable enough to be isolated; thus, the half-life of ES^2 is only 13 min. The time course of the formation of the isolated intermediate was measured (Figure 12); the rate constant, 0.015 min^{-1}, equalled k_4 (0.0148 min^{-1} at −64 °C). The rate constant k_4 then is assigned to the step interconverting ES^2 and ES^3, and so k_5 refers to the last step, thus resolving the ambiguity in evaluating k_4 and k_5.

Some light was thrown on the nature of the intermediates by their instability to acid. A reaction mixture at −65 °C was acidified to pH* >2 with 6 M HCl in 60% (v/v) methanol after 3 min, 30 min, or 6 h, times chosen so that ES^1, ES^2, or ES^3 predominated. The samples were either warmed to 4 °C and fractionated on Sephadex G-25 in 40% (v/v) acetic acid or fractionated at −65 °C on Sephadex LH-20 at pH* 2. In no case did low molecular weight material (measured by A_{500}) coelute with enzyme. These results suggest that all three intermediates are noncovalent complexes.

Discussion

Validity of Results from Cryoenzymology of β-Lactamase II. The Arrhenius plots for the hydrolysis of benzylpenicillin and of nitrocefin lacked discontinuities, and the apparent energies of activation in water and cryosolvents were similar (Table I). Moreover, the branched pathway for the hydrolysis of benzylpenicillin by manganese β-lactamase II was operative at ordinary temperatures and in water. Thus, the doubts that the mechanism deduced from results obtained in cryosolvents may be peculiar to those conditions may be allayed.

Nature of Intermediates. The experiments described in the present paper show that the intermediates that accumulate during the hydrolysis by β-lactamase II of benzylpenicillin, and of nitrocefin, are the noncovalent Michaelis complex ES^1 and variants that are likely to be conformers. The low-temperature acid quench of the hydrolysis of benzylpenicillin (Table IV) provided particularly clear evidence that the intermediate that had accumulated was an enzyme–substrate complex. This method might usefully be applied to other enzymes, e.g., carboxypeptidase A, where Galdes et al. (1983) have concluded that there was no evidence for a covalent acyl-enzyme intermediate. The Michaelis complex from nitrocefin and zinc β-lactamase II provided information about the environment of the bound substrate. Here, there was no change in the visible spectrum when ES^1 accumulated. The intermediates in the branched pathway of nitrocefin hydrolysis differed in this respect: in ES^3 the environment of the chromophore resembled that of substrate, but in ES^2 λ_{max} shifted to longer wavelength as if the dinitrophenyl group were "tucked in". Similarly, in the branched pathway of benzylpenicillin hydrolysis by cobalt β-lactamase II, there was a change in fluorescence (enhanced emission, excitation at 280 nm) as ES^1 was converted into ES^2. The electronic absorption spectra of the ES^1 and ES^2 intermediates in the hydrolysis of benzylpenicillin by cobalt(II) β-lactamase II confirm the central role of the metal in catalysis and provide information about its environment during turnover. The electronic absorption spectrum of cobalt (II) β-lactamase II shows a charge-transfer band at 343 nm arising from ligation of the catalytic metal by the single cysteine residue of the enzyme. The absorption has an unusually low extinction coefficient for a cobalt(II)–sulfur charge-transfer band. By contrast, the charge-transfer absorbance is both greatly enhanced (7-fold increase) and of lower λ_{max} (333.4 nm) in ES^1. The decrease in λ_{max} indicates a strengthening of cysteine–cobalt(II) bond upon formation of ES^1 and probably reflects a general tightening of the metal coordination sphere relative to that of the free enzyme. The cysteine ligand is not displaced during catalysis.

Nature of Active Site. Information about the active site of β-lactamase II has come from spectroscopy, ^1H NMR spectroscopy of the zinc and cobalt enzymes, and electronic spectroscopy of the cobalt enzyme (Davies & Abraham, 1974; Baldwin et al., 1980). The visible spectrum suggests some similarity between carbonic anhydrase and β-lactamase II. Thus, cobalt carbonic anhydrase B at high pH closely resembles cobalt β-lactamase II both in absorption spectrum and in magnetic circular dichroic spectrum (Coleman, 1965; Holmquist et al., 1975; Baldwin et al., 1980b). There are characteristically well-separated peaks at 620 and 640 nm, rather reminiscent of pentacoordinate Co(II) complexions. These peaks are lost when carboxylates and some other anions bind (Lindskog, 1966; Taylor et al., 1970; Bertini & Luchinat, 1983). Now the ligands to the metal atom in carbonic anhydrase are three histidine residues, two of which are in a His-X-His sequence, and a water molecule (Kannan et al., 1977). The enzyme ligands to the metal in β-lactamase II are believed, from spectroscopic evidence, to be three histidine residues and the thiol group (Baldwin et al., 1980b), and here also two of the histidine residues are in a His-X-His sequence (Baldwin et al., 1979; Ambler, 1980). The presence of a metal-coordinated water molecule as a fifth ligand) is yet to be proved but may reasonably be expected from analogy with other zinc hydrolases and the pentacoordination of the metal suggested by the MCD spectrum of cobalt(II) β-lactamase II. The well-separated peaks at 614 and 638 nm in the spectrum of cobalt β-lactamase II are absent from the spectrum of the obligatory, noncovalent intermediate ES^1. This parallels the change on inhibitor binding to carbonic anhydrase B referred to above. In the absence of sulfur ligands to cobalt(III), the spectral intensity of the $d \rightarrow d^*$ transitions is a reasonably good indicator of coordination geometry, either four/five or six, for six-coordinate complexes have an exceptionally weak absorption with ϵ values never greater than 100 M^{-1} cm^{-1}. With sulfur ligands this is not so, and asymmetric six-coordinate complexes may have ϵ values of several hundred (Banci et al., 1982). It follows that deductions concerning the geometry of the metal ion in ES^1 and ES^2 are not possible from visible spectra alone.

Group modification has recently provided evidence for an essential glutamate residue in β-lactamase II (Little et al., 1985). This residue may well play the same role as Glu-143 in thermolysin (Mozingo & Matthews, 1984) and act as a proton shuttle, the proton withdrawn from the attacking water molecule being transferred to the nitrogen atom, a fairly common feature in enzymic catalysis; e.g., similar roles are played in an aldolase (Meloche & Glusker, 1973) and an isomerase (Alber et al., 1981).

Mechanism of Action of β-Lactamase II. The nonenzymic hydrolysis of β-lactams is catalyzed by metal ions; the carboxylate group and the β-lactam nitrogen atom of benzylpenicillin coordinate to copper(II), which stabilizes the transition state for hydrolysis by 14 kcal/mol (Page, 1984). Catalysis is due to the enhanced basicity of the nitrogen atom in the transition state. The direction of nucleophilic attack on the β-lactam ring is from the less hindered α side, although stereoelectronic control would favor β-side attack (Deslongchamps, 1983; Page, 1984). In β-lactamase II the attacking group may also approach from the less hindered α side

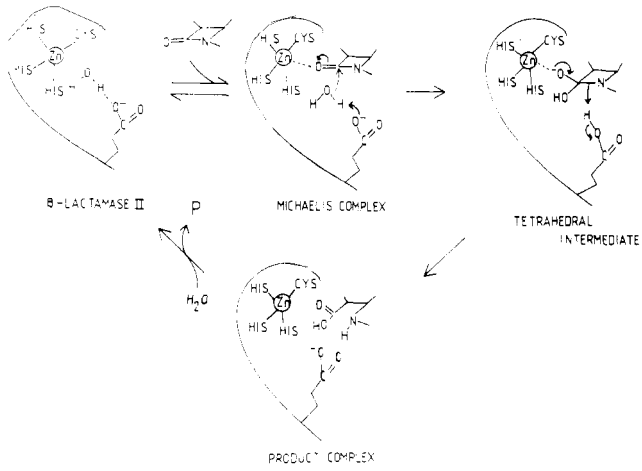

FIGURE 13: Groups that may interact in catalysis by β-lactamase II.

for a wide range of (β-lactam) substrates are hydrolyzed at high, and somewhat comparable, rates, regardless of the size of the side-chain substituents; e.g., methicillin (a penicillin with a bulky side chain) is hydrolyzed even more rapidly than benzylpenicillin. The similarity of the environment of the chromophore in unbound nitrocefin and when bound as ES^1 (and ES^3) also suggests that the cephalosporin 3′ side chain is not deeply buried in the active site.

An attractive mechanistic possibility is that either the oxygen atom or the nitrogen atom of the β-lactam displaces the water molecule coordinated to the metal as a fifth ligand and the metal acts as an electrophilic catalyst. The essential glutamate mentioned above probably functions as a general base and deprotonates the water molecule that attacks the β-lactam carbonyl group (Figure 13). In a second mechanism, the zinc ion does not interact directly with the substrate; instead, the water molecule coordinated to the metal attacks the β-lactam. A third possibility allows for six-coordinate zinc, with both substrate and water binding to the metal. This might not occur in ES, but only at a later stage; in the mechanism for peptide bond cleavage by thermolysin, substrates do not bind directly to the zinc in the Michaelis complex, but the substrate penetrates more deeply into the active site as the tetrahedral intermediate is approached (Hangauer et al., 1984). The metal ligands in β-lactamase II may be so disposed that metal binding in the six-coordinate transition states leading to (and from) the tetrahedral intermediate is favored and binding in the enzyme itself is less favorable, hence the high metal dissociation constants, 140 or 0.7 μM for cobalt or zinc, respectively, and the low extinction coefficient for the charge-transfer band (Baldwin et al., 1980b). A fourth possibility is that the zinc-bound thiol group acts as a nucleophile. This seems unlikely, since the reactivity of the thiol would be lessened when bound to metal.

Significance of Branched Pathways. Branched pathways may be a consequence of the fluctuations in structure that all proteins undergo (Cooper, 1984). The energies of activation for the branching steps (4–11 kcal/mol) are comparable with the changes in enthalpy expected for segmental unfolding (Privalov, 1979; Englander & Kallenbach, 1984). A consequence of the branching steps having relatively low E_a values is that at ordinary temperatures branching is diminished relative to turnover.

Substrate-Induced Deactivation of β-Lactamase II by Cephalosporins. The rate of hydrolysis of certain cephalosporins by zinc β-lactamase II decreases progressively; this is due neither to depletion of substrate nor to inhibition by product (Davies, 1974) and is to date restricted to cephalosporins that have a leaving group at the exocyclic C-3 methylene residue (Abraham & Waley, 1979). The departure of the leaving group is catalyzed by β-lactamase II (Faraci & Pratt, 1984). The deactivation may be the result of the progressive accumulation of a noncovalent enzyme–substrate complex formed by a branched pathway of the type that we have demonstrated.

Registry No. Nitrocefin, 41906-86-9; benzylpenicillin, 61-33-6; β-lactamase, 9073-60-3.

REFERENCES

Abraham, E. P., & Waley, S. G. (1979) in *The β-Lactamase* (Hamilton-Miller, J. M. T., & Smith, J. T., Eds.) pp 311–338, Academic Press, London.

Alber, T., Banner, D. W., Bloomer, A. C., Petsko, G. A., Phillips, D. C., Rivers, P. S., & Wilson, I. A. (1981) *Philos. Trans. R. Soc. London, B 293*, 159–171.

Ambler, R. P. (1980) *Philos. Trans. R. Soc. London, B 289*, 321–331.

Auld, D. S., Galdes, A., Geoghegan, K. F., Holmquist, B., Martinelli, R. A., & Vallee, B. L. (1984) *Proc. Natl. Acad. Sci. U.S.A. 81*, 5041–5045.

Baldwin, G. S., Waley, S. G., & Abraham, E. P. (1979) *Biochem. J. 179*, 459–463.

Baldwin, G. S., Edwards, G. F. StL., Kiener, P. A., Tully, M. J., Waley, S. G., & Abraham, E. P. (1980a) *Biochem. J. 191*, 111–116.

Baldwin, G. S., Galdes, A., Hill, H. A. O., Waley, S. G., & Abraham, E. P. (1980b) *J. Inorg. Biochem. 13*, 189–204.

Banci, L., Bencini, A., Benelli, C., Gatteschi, P., & Zanchini, C. (1982) *Struct. Bonding (Berlin) 52*, 37–86.

Barshop, B. A., Wrenn, R. F., & Frieden, C. (1983) *Anal. Biochem. 130*, 134–145.

Bertini, I., & Luchinat, C. (1983) *Acc. Chem. Res. 16*, 272–279.

Bicknell, R., Knott-Hunziker, V., & Waley, S. G. (1983) *Biochem. J. 213*, 61–66.

Bicknell, R., Cartwright, S. J., Emanuel, E. L., Knight, G. C., & Waley, S. G. (1985) *Recent Advances in the Chemistry of β-Lactam Antibiotics* (Brown, A. G., & Roberts, S. M., Eds.) pp 280–292, Royal Society of Chemistry, London.

Charnas, R. L., & Knowles, J. R. (1981) *Biochemistry 20*, 2732–2737.

Coleman, J. E. (1965) *Biochemistry 4*, 2644–2655.

Cooper, A. (1984) *Prog. Biophys. Mol. Biol. 44*, 181–214.

Cornish-Bowden, A., & Eisenthal, R. (1978) *Biochim. Biophys. Acta 523*, 268–272.

Davies, R. B. (1974) D. Phil. Thesis, University of Oxford.

Davies, R. B., & Abraham, E. P. (1974) *Biochem. J. 143*, 129–135.

Davies, R. B., Abraham, E. P., & Melling, J. (1974) *Biochem. J. 143*, 115–127.

Deslongchamps, P. (1983) *Stereoelectronic Effects in Organic Chemistry*, pp 158–160, Pergamon Press, Oxford.

Douzou, P. (1977) *Cryobiochemistry: An Introduction*, Academic Press, New York.

Douzou, P., Hui Bon Hoa, G., Maurel, P., & Travers, F. (1976) in *Handbook of Biochemistry and Molecular Biology* (Fasman, G. D., Ed.) 3rd ed., pp 520–540, Chemical Rubber Publishing Co., Cleveland, OH.

Dreyfus, M., Vandenbunder, B., & Buc, H. (1978) *FEBS Lett. 95*, 185–189.

Englander, S. W., & Kallenbach, N. R. (1984) *Q. Rev. Biophys. 16*, 521–655.

Faraci, W. S., & Pratt, R. F. (1984) *J. Am. Chem. Soc. 106*, 1489–1490.

Galdes, A., Auld, D. S., & Vallee, B. L. (1983) *Biochemistry 22*, 1888–1893.
Hangauer, D. G., Mozingo, A. F., & Matthews, B. W. (1984) *Biochemistry 23*, 5730–5741.
Hill, H. A. O., Sammes, P. G., & Waley, S. G. (1980) *Philos. Trans. R. Soc. London, B 289*, 333–344.
Holmquist, B., Kaden, T. A., & Vallee, B. L. (1975) *Biochemistry 14*, 1454–1461.
Kannan, K. K., Petef, M., Fridborg, K., Cid-Dresdner, H., & Lorgren, S. (1977) *FEBS Lett. 73*, 115–119.
Knott-Hunziker, V., Petursson, S., Waley, S. G., Jaurin, B., & Grundstrom, T. (1982) *Biochem. J. 207*, 315–322.
Lindskog, S. (1966) *Biochemistry 5*, 2641–2646.
Little, C., Emanuel, E., Gagnon, J., & Waley, S. G. (1985) *Biochem. J.* (in press).
Maurel, P. (1978) *J. Biol. Chem. 253*, 1677–1683.
Meloche, H. P., & Glusker, J. P. (1973) *Science (Washington, D.C.) 181*, 350–352.
Mozingo, A. F., & Matthews, B. W. (1984) *Biochemistry 23*, 5724–5729.
O'Callaghan, C. H., Morris, A., Kirby, S. M., & Shingler, A. H. (1972) *Antimicrob. Agents Chemother. 1*, 283–288.
Page, M. I. (1984) *Acc. Chem. Res. 17*, 144–151.
Pratt, R. F., & Govardhan, C. P. (1984) *Proc. Natl. Acad. Sci. U.S.A. 81*, 1302–1306.
Privalov, P. L. (1979) *Adv. Protein Chem. 33*, 167–241.
Rodiguin, N. M., & Rodiguina, E. N. (1964) *Consective Chemical Reactions*, pp 111–131, Van Nostrand, Princeton, NJ.
Sabath, L. D., & Abraham, E. P. (1966) *Biochem. J. 98*, 11c–13c.
Saino, Y., Kobayashi, F., Inoue, M., & Mitsuhashi, S. (1982) *Antimicrob. Agents Chemother. 22*, 564–570.
Selwyn, M. J. (1965) *Biochim. Biophys. Acta 105*, 193–195.
Tan, H., & Lovrien, R. (1972) *J. Biol. Chem. 247*, 3278–3285.
Taylor, P. W., King, R. W., & Burgen, A. S. V. (1970) *Biochemistry 9*, 3894–3902.
Vallee, B. L., & Galdes, A. (1984) *Adv. Enzymol. Relat. Areas Mol. Biol. 56*, 283–430.
Wharton, C. W., & Szawelski, R. J. (1982) *Biochem. J. 203*, 351–360.

NMR Studies of Chromomycin A_3 Interaction with DNA†

Elisha Berman,*,‡ Stephen C. Brown,§ Thomas L. James,§ and Richard H. Shafer*,§

Department of Pharmaceutical Chemistry, School of Pharmacy, University of California, San Francisco, California 94143, and Department of Organic Chemistry, The Weizmann Institute of Science, 76100 Rehovot, Israel

Received February 14, 1985

ABSTRACT: The binding of chromomycin A_3 to calf thymus DNA and poly(dG-dC) has been studied by ^{13}C and ^{1}H NMR with emphasis on the mode of binding, the role of Mg^{2+}, and pH effects. The most prominent changes in the DNA base pair ^{13}C NMR resonances upon complexation with chromomycin were observed for G and C bases, consistent with the G-C preference exhibited by this compound. Comparison of the ^{13}C spectrum of DNA-bound chromomycin A_3 with that of DNA-bound actinomycin D, a known intercalator, showed many similarities in the base pair resonances. This suggested the possibility that chromomycin A_3 binds via an intercalative mechanism. ^{1}H NMR studies in the imino proton, low-field region of the spectrum provided additional evidence in support of this binding mode. In the low-field spectrum of chromomycin A_3 bound to calf thymus DNA, a small shoulder was observed on the upfield side of the G-C imino proton peak. Similarly, in the chromomycin A_3 complex with poly(dG-dC), a well-resolved peak was found upfield from the G-C imino proton peak. These results are expected for ligands that bind by intercalation. Futhermore, in both the calf thymus and poly(dG-dC) drug complexes (in the presence of Mg^{2+}) a broad peak was also present downfield ($\sim$16 ppm from TSP) from the DNA imino protons. This was attributed to the C-9 phenolic hydroxyl proton on the chromomycin chromophore. Visible absorbance spectra at different pH values showed that the role of Mg^{2+} in the binding of chromomycin A_3 to DNA is more than simple neutralization of the drug's anionic change.

Chromomycin A_3, an antitumor antibiotic that belongs to the aureolic acid group (Remers, 1979), is composed of the aglycon chromomycinone and five sugar units consisting of chromoses A, B, C, and D (Miyamoto et al., 1967). The complete structure of chromomycin A_3 (structure **1**) was established only recently by ^{1}H and ^{13}C NMR spectroscopy (Thiem & Meyer, 1979). It is of importance to note that the chromophore has a pK_a of $\sim$7.0 and that divalent cations, in particular Mg^{2+}, are needed for the strong interaction of the drug with DNA to take place (Hayasaka & Inou, 1969; Nayak et al., 1973). It was also found that chromomycin A_3 shows a preference of G-C base pairs in DNA (Behr et al., 1969; Berman & Shafer, 1983; Van Dyke & Dervan, 1983) and that the sugar side chains play a role in the binding to DNA (Behr et al., 1969; Berman & Shafer, 1983). Similar properties were observed for related members of the aureolic acid group such

† This work was supported by U.S. Public Health Service Grant CA 27343 awarded by the National Institutes of Health, DHHS (R.H.S.), and a grant from the Cancer Research Coordinating Committee of the University of California (E.B.).
‡ The Weizmann Institute of Science.
§ University of California.

0006-2960/85/0424-6887$01.50/0